Advanced Steel Construction – Vol. 16 No. 4 (2020) 328–336
DOI:10.18057/IJASC.2020.16.4.5

EXPERIMENTAL INVESTIGATION ON TEMPERATURE EVOLUTION OF STEEL BEAMS IN NATURAL FIRES

Er-Feng Du [1], Gan-Ping Shu [1, *], Yi-Qun Tang [1], Ying Qin [1], Xiao Lyu [2] and Zhong Zhou [1]

[1] *Key Laboratory of Concrete and Prestressed Concrete Structures of Ministry of Education, School of Civil Engineering, Southeast University, Nanjing, China*

[2] *School of Civil Engineering, Shandong Jianzhu University, Ji'nan, China*

** (Corresponding author: E-mail: shuganping@seu.edu.cn)*

ABSTRACT

This paper presents an experimental project of a 3D steel portal frame subjected to a natural fire to investigate the evolution of temperatures of the hot gas layer and the steel beams. Temperature evolution of the steel beams during the test was recorded and compared with those calculated by current design codes, i.e. Eurocode EN 1993-1-2 and Chinese Code CECS200. The experimental results revealed that the temperature of the hot gas gradually decreased with the distance from the fire source, and the temperature variations in the steel beams had obvious hysteresis compared to those of the hot gas. The results calculated according to the equations specified by EN 1993-1-2 and CECS200 were very similar. However, there were noticeable differences between the calculated data and the experimental results after the temperature of the steel beam was higher than 600°C. The calculation for the temperature of steel beams in the hot gas layer does not need additional consideration of the thermal radiation from the flame. Based on the experimental results, this paper improves the equations specified in EN 1993-1-2, using correction coefficients of convection and radiation. It is found that the modified method obtains calculation results in satisfactory agreement with the experimental results, thereby providing a reference for predicting the temperature of steel beams in natural fires.

ARTICLE HISTORY

Received: 3 June 2020
Revised: 5 September 2020
Accepted: 6 September 2020

KEYWORDS

Experimental study;
Steel beam;
Hot gas;
Temperature;
Natural fire

1. Introduction

Large-space steel structures are extensively utilized in public buildings, such as stadiums, airports, industrial plants, et al. Abundance research has been conducted on the structural performance and construction methods of these structures at ambient temperature [1-4]. In recent years, the fire resistance and the design method of large-space steel structures have become crucial issues concerned by researchers and engineers. Lu et al. [5] analysed the fire performance of a large exhibition centre in different fire scenarios and proposed recommendations on the fire-resistance design of large-space steel truss structures. Du et al. [6] proposed an analytical method to capture the transient tension force in a pre-tensioned steel cable subjected to localized fires. Woźniczka [7] investigated the effects of different factors on the fire resistance of long-span truss girders during the fire growth and decay phases, and the results showed that the fireproof insulation of the structure can be reduced. Liu et al. [8] explored the mechanical response of welded hollow spherical joints at elevated temperatures through experimental and numerical studies, and provided a simplified calculation formula to predict the bearing capacity of the joints at high temperatures. Jiang et al. [9] conducted fire tests on a full-scale roof structure having six main steel trusses in non-destructive and destructive manners, and obtained the failure modes and deformation curves in natural fires of the structure. Some scholars performed experimental studies and finite element analyses on the mechanical behaviours of different forms of steel portal frame structures under natural fires [10-14].

In general, fires occurring in large-space steel structures will localize rather than flashover. The temperature field of the whole building is not uniform, which is quite different from compartment fires. Thus, the traditional fire-resistance design method under standard fire conditions is unsuitable for large-space steel structures, and investigations on the performance-based design method should be conducted. The performance-based fire-resistance design method involves the consideration of a natural fire model based on the fire load, the geometrical size of the building, mechanic properties of steel at elevated temperatures, the temperature distribution in structural members and the response of the entire structural system under fires [15, 16].

To implement the performance-based fire-resistance design, a rational calculation method for the temperature evolution of structural members under natural fires is crucial. For large-space structures under natural fires, the space inside the building can be divided into three regions, including the flame region, the region of the hot gas layer, and the region under the hot gas layer. The heat-transfer mechanisms are different in these three regions, and thus the temperature development laws for structural members in these three regions are also different. According to the Chinese code CECS200 [17], the specified equation for the temperature rise of structural members is based on the standard fires. In terms of the European codes including EN 1991-1-2 [18] and EN 1993-1-2 [19], localized fire is specified, but its calculation method is inconvenient to use in practice since the temperature of the fire plume varies in the vertical direction.

Regarding the calculation methods for the temperature of structural members under natural fires, Latham et al. [20] experimentally investigated the temperature of steel members exposed to natural fires in a compartment. The test data were then used for estimating the structural response, by the equivalent time of fire exposure. Wong et al. [21] and Ghojel [22] studied the factors that may affect the temperature evolution of steel members under compartment fires, and proposed calculation models for the temperature rise of members, which took into account the absorption of flame radiation by the heat-transfer medium. Then the calculation models were experimentally verified. Wald et al. [23, 24] conducted compartment fire tests on buildings with full-scale steel frames. The temperature of the steel member was measured and compared with the results predicted by the calculation methods given in Eurocodes.

Based on the lumped differential formulation, Du and Li [25] presented a calculation method for the temperature rise of steel members under large-space fires, with consideration of the effect of flame radiation. They also proposed a limit value for the radiation shape factor based on the parametric analysis. By using the heat balance equation, Huang et al. [26] proposed a simplified calculation method for the temperature development of steel members in large-space fires. The influence of flame radiation was considered based on the parametric analysis. Meanwhile, a critical value of the building height was also suggested for the cases where the flame radiation effect was neglected. Zhang et al. [27] used the adiabatic surface temperature method to establish a simple heat transfer model of steel members under localized fires, and the results of the proposed model were close to those from the FDS (Fire Dynamics Simulator) simulation. Based on a point-source model, Zhang et al. [28] established a modified method for predicting the temperature rise of steel members, with consideration of the effect of flame radiation. An experimental study was performed on the temperature elevating process of a steel beam under a localized fire in a large space. The calculation results were found, by comparison, to be in satisfactory agreement with the experimental data.

In summary, the studies on the calculation methods for temperature evolution of steel members under natural fires are limited. Moreover, in the experiment conducted by Zhang et al. [28], the power of the fire source was small and the resulting temperatures of steel members were low. Additionally, the cooling period was not considered in the calculation methods proposed by the previous researches. Thus, it is necessary to perform more typical experiments in this research field.

To solve the aforementioned problems, a model of a portal frame building was designed and constructed in this study. A fire test was performed on the model to investigate the development of the natural fire, and the temperature distribution of the hot gas layer and the steel beams under the fire. Results obtained by the equations for the temperature evolution of steel beams specified by CECS200 and EN 1993-1-2 were compared to the experimental results, to validate the applicability of the equations under natural fires.

2. Experimental program

2.1. Introduction of the test model

The test model was a single compartment which covered an area of 6 by 12.5m as shown in Figs. 1 and 2. The columns were 2.25m high and the roof was inclined at 1/10. A total of six portal frames were spaced apart at an interval of 2.5m and the configuration of a representative frame is indicated in Fig. 3. The section of the beams and columns was H80×50×4.5×6.5mm. Roof purlins and wall purlins were bent from the galvanized steel sheet to form a section of C60×38×12×1.6mm. To ensure the safety of the beam-column connections before member failures, fully-welded connections at the beam ends were adopted and end-plate connections for the beam splices were applied at a distance of 0.8m from the column flange, as shown in Fig. 4.

Fig. 1 Steel portal frame building for the fire test

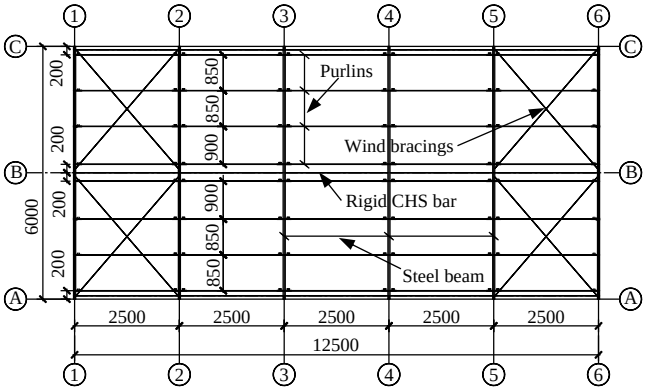

Fig. 2 Plan view of the roof structure (mm)

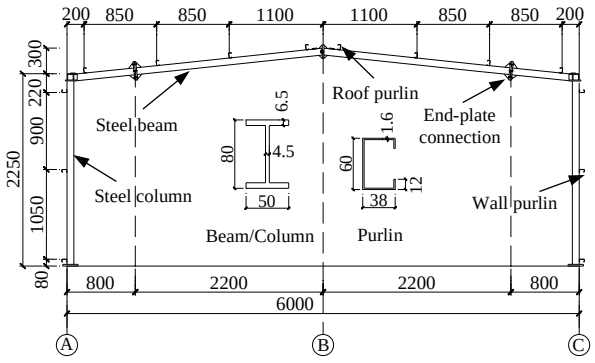

Fig. 3 Elevation view of the portal frame (mm)

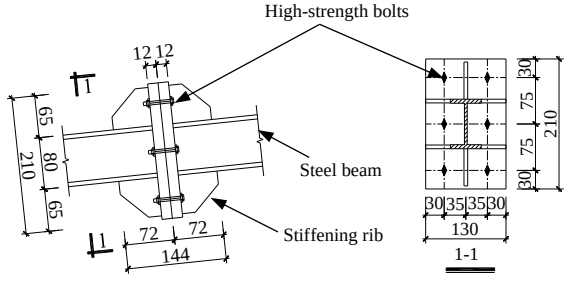

Fig. 4 End-plate connection for beam-to-beam joint (mm)

The purlins were connected to the beams and columns with M10 bolts, and knee braces of the roof purlins were used to prevent the out-of-plane buckling. Rigid bars (CHS42×3) were arranged between the ridges and the beam-column connections. Steel bars (Φ10) were employed as wind bracings in the outer spans. The roof cladding was made of 75mm thick composite panels with rock wool insulation, while the wall cladding was made of 0.5mm thick single-layered profiled steel sheets. The steel grade was Q235.

Each gable wall contained a 2.03m high and 1.2m wide door opening. Along Axis A, three window openings with a height of 0.9m were designed in the facade wall as plotted in Fig. 5. Cesium-potassium monolithic flameproof glass was installed in the middle window, while common glass was installed in the other two windows labelled with a, b. The flameproof glass was arranged for the convenience of observation during the test. Along Axis C, there were only two windows labelled with c and d in the wall, with common glass installed.

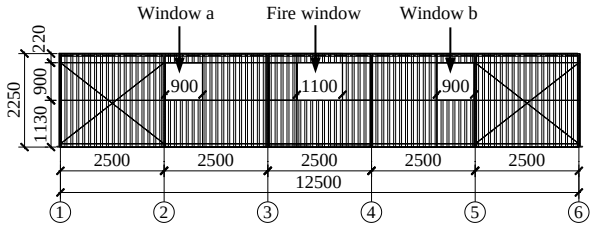

Fig. 5 Elevation view along Axis A (mm)

The concrete bases with a length of 0.7m, a width of 0.7m and a height of 0.6m supported the columns. The concrete grade was C25 and the columns of the main frames were designed to be pinned at the base with two anchor bolts (M20).

2.2. Fire source

A natural fire source was set up below the steel beam along Axis 3 as indicated in Fig. 6. The fire source consisted of six 0.7×0.7m oil pans each containing 11kg diesel. The amount of the fuel was designed to achieve a representative fire in an industrial building, based on the data from fire tests recorded in the literatures and simulation results from the software FDS [29]. To concentrate the heat on the rafters, the oil pans were raised to a height of 1.15m above the ground level by a supporting platform.

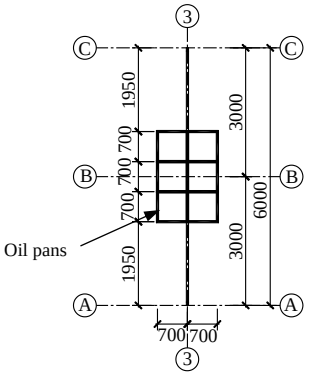

Fig. 6 Arrangement of the fire source (mm)

2.3. Setup of temperature measurement

Type-K thermocouples were adopted for measuring the temperatures of hot gas and steel members. The temperature data were collected by the data acquisition instrument TDS303. Fig. 7 shows positions of the thermocouples in the frame along Axis 3. The name of the thermocouple contains 3 parts, including “S” or “G”, the number of the axis and the number of the thermocouple, in which S and G represent the steel member and the hot gas, respectively. The thermocouples measuring the hot gas were arranged at a distance of 50mm from the member surface. To obtain the temperature distribution in the particular sections of the eaves and the ridge, the thermocouples were located at the top, mid-web and bottom flanges, as plotted in sections a and b.

For the other sections, each has only one thermocouple located at the mid-web.

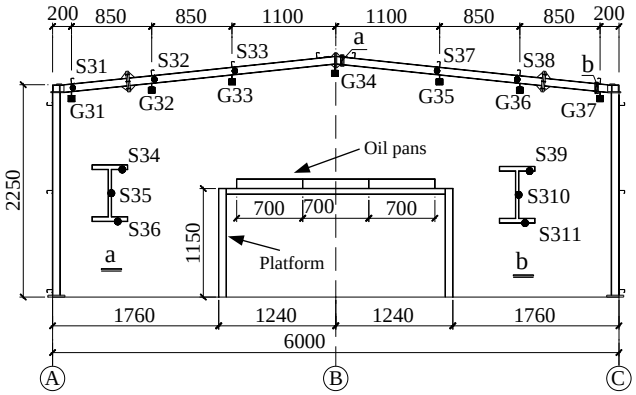

Fig. 7 Positions of thermocouples along Axis 3 (mm)

In terms of the other portal frames, the number of thermocouples was less than that along Axis 3. The setup of thermocouples at the eaves and the ridge was similar to Axis 3 except that only one thermocouple was located at the mid-web of the steel beam in the other portal frames, as plotted in Fig. 8. The number "0" in the plot means that no steel thermocouple was arranged for eaves along Axes 1 and 6.

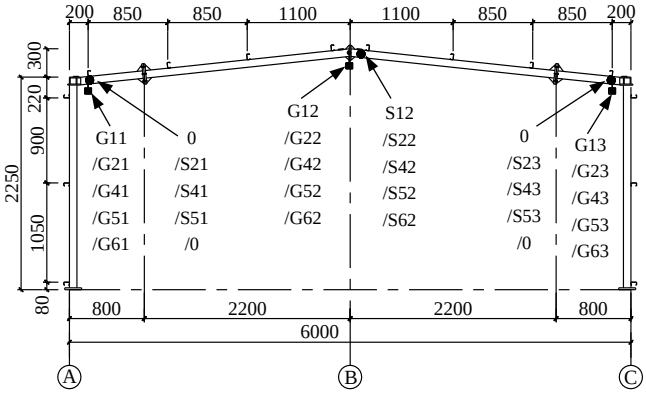

Fig. 8 Positions of thermocouples along Axes 1/2/4/5/6 (mm)

3. Experimental results

3.1. Visual observation and discussion

The middle two oil pans burned first following the ignition at the beginning of the test, and the other oil pans burned at 1min 25s after the ignition. A thick layer of smoke formed beneath the roof, with a large amount of smoke

Fig. 9 Test building in the fire (1min 25s)

Fig. 10 Test building in the fire (5min 56s)

Fig. 11 Test building in the fire (10min 19s)

Fig. 12 Test building in the fire (13min 20s)

emitting from the door openings, as shown in Fig. 9. Dark smoke spread out of the building at 2min 50s. At 5min 56s, the oil source blazed fiercely and the flame spread around the edge of oil pans, as plotted in Fig. 10. As shown in Fig. 11, the fire began to abate without flame spilling at 10min 19s. At 11min 20s, the smoke above the roof decreased greatly. At 13min 20s, fire in the middle oil pans almost extinguished, as plotted in Fig. 12. Then, the flame extinguished at 16min 58s. Moreover, at the initial stage of the test, a noise of "bang, bang" was heard sometimes. During the intermediate stage of the test, some flames emitted out of the roof through the sheet joints above the fire source.

(a) Window a

(b) Window b

(c) Window c

(d) Window d

Fig. 13 Windows with common glass after the fire test

Along Axis A, the corners of windows a and b cracked at 3min 16s and 3min 53s respectively after the ignition. At 4min 53s, the cracks in the corners of window a further expanded and some glass debris fell. A large crack occurred in window b and some glass debris fell at 5min 21s. At 6min 28s, most of the glass in window a dropped down and a sizable flame run out. The cracks in the corners of window c expanded seriously at 7min 50s. A great part of the glass in window b broke at 8min 55s. During the entire test, only tiny cracks appeared in window d. The windows with common glass after the test are shown in Fig. 13, while the fire-resistant glass was kept intact during the whole process of the fire test.

3.2. Temperature evolution and analysis

The temperature-time relationship of the hot gas below the steel beam along Axis 3 is plotted in Fig. 14. It can be seen that the temperature of the hot gas (G32-G36) above the fire source generally experienced three periods: a growth period, a fully developed period, and a decay period. The temperature rose fast during the first period, and then kept nearly constant or grew slowly in the second period. At the beginning of the third period, the temperature decreased rapidly. When the temperature dropped to 300ºC, it began to decline slowly. The highest gas temperature was found by the thermocouple G34 around the roof ridge right above the fire source, and its peak value was 1182.7ºC. The graph also indicates that the temperature of hot gas decreased from the roof ridge to the eaves. In general, the temperature distributed symmetrically on both sides of the roof ridge.

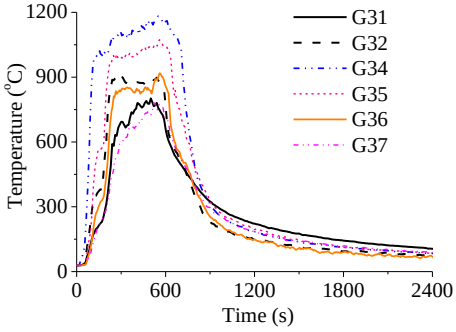

Fig. 14 Temperature of the gas near the beam along Axis 3

Figs. 15-17 show the temperature distribution of the hot gas near the ridge and the eaves along Axes A and C, respectively. It can be seen that the peak temperature declined from the span of Axis 3 to the other spans on both sides.

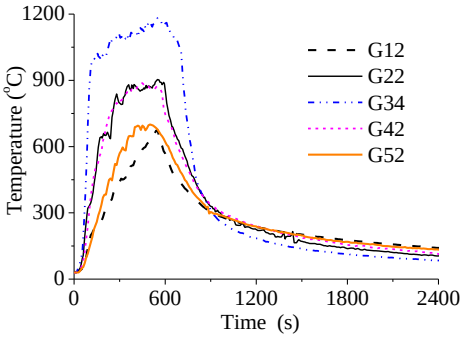

Fig. 15 Temperature of the gas near the ridge

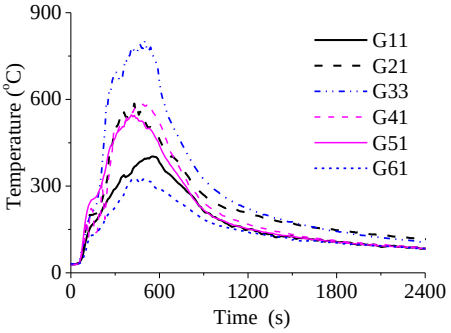

Fig. 16 Temperature of the gas near the eave along Axis A

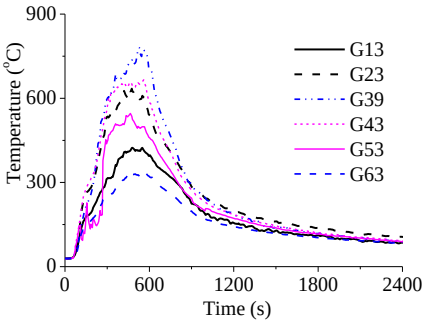

Fig. 17 Temperature of the gas near the eave along Axis C

The temperature-time curves for the top, mid-web and bottom flanges of the steel beam at the roof ridge (section a) along Axis 3 are shown in Fig. 18. It can be seen that the temperature distribution in the beam section was normally uniform, because the steel had sound conductivity and the beam section was entirely surrounded by the flame. During the heating period, the temperature of the beam was lower than that of the hot gas. The peak temperature of the steel beam reached 941ºC. During the cooling period, in turn, the temperature of the beam was much higher than that of the gas. Fig. 19 illustrates the temperature against time for the steel beams at the eave (section b) along Axis 3. The peak temperature reached about 600ºC and the temperature evolution law was similar to that in section a.

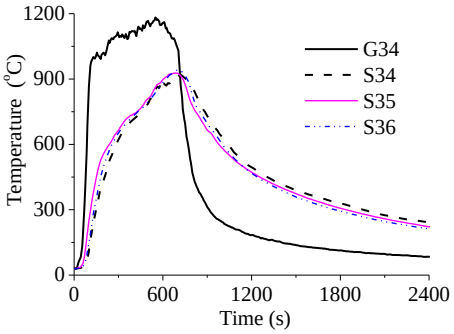

Fig. 18 Temperature histories for the ridge along Axis 3

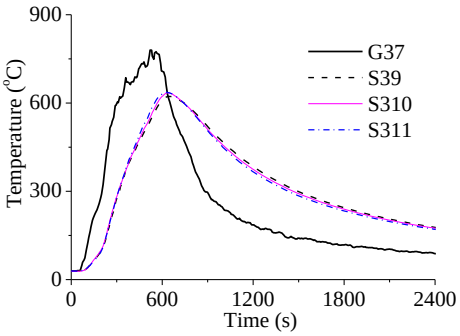

Fig. 19 Temperature histories for eaves along Axis 3

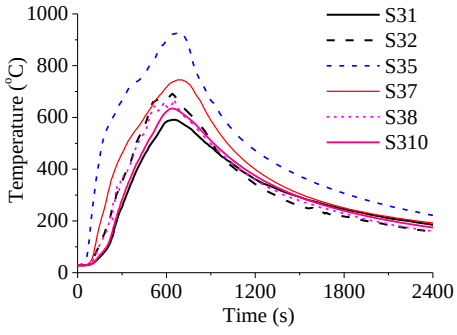

Fig. 20 Temperature of the beam along Axis 3

The temperature-time curves for the web of the steel beam along Axis 3 are plotted in Fig. 20. According to the measurement, the roof ridge had the highest temperature, and the temperature decreased gradually towards the two eaves.

Figs. 21-23 illustrate temperature-time curves for the webs of the beams at the roof ridge and the eaves along Axes A and C. As shown in Fig. 21, the peak temperature decreased from the span of Axis 3 to the other spans. Figs. 22-23 show that the peak temperature of the steel beam at the eave of Axis 4 was higher than that of Axis 2 since the position of Axis 4 was farther from the door opening than Axis 2. The peak temperature of the steel beam at the eave of Axis C was higher than that of Axis A because the window near Axis A was damaged greatly, leading to a great loss of heat. Due to the failure of thermocouples for measuring points G33, G62, S22 and S33, the corresponding temperature curves are not given here.

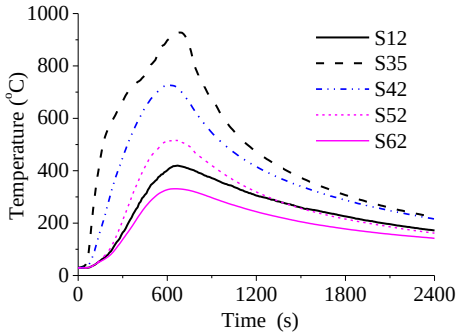

Fig. 21 Temperature of the beam at the ridge

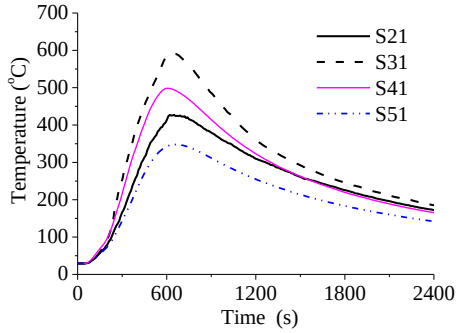

Fig. 22 Temperature of the beam at the eave along Axis A

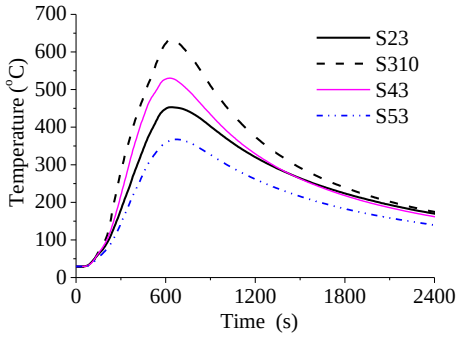

Fig. 23 Temperature of the beam at the eave along Axis C

4. Temperature calculation of steel beams

In this section, the equations for temperature variations of steel members under standard fires, specified by EN 1993-1-2 and CECS200, are assessed for the applicability in natural fires.

4.1. Calculation Method

4.1.1. EN 1993-1-2 Equation

The following equation for calculating the temperature of unprotected steel members under fires is provided by EN 1993-1-2:

$$\Delta T_a = k_{sh} \frac{A_m / V}{c_a \rho_a} h_{net} \Delta t \tag{1}$$

where ΔT_a is the temperature increment of a steel member [°C]; k_{sh} is the correction factor for the shadow effect; A_m/V is the section factor for the unprotected steel member [1/m], in which A_m is the surface area of the member per unit length [m^2/m] and V is the volume of the member per unit length [m^3/m]; ρ_a and c_a are the density and specific heat of steel, respectively, in which ρ_a=7850 kg/ m^3, and c_a=600 J/(kg·°C); h_{net} is the design value of net heat flux per unit area [W/m^2]; and Δt is the time interval and should not be more than 5 seconds.

h_{net} is determined by

$$h_{net} = h_{net,c} + h_{net,r} \tag{2}$$

where $h_{net,c}$, and $h_{net,r}$ are the net convective heat flux (W/m^2) and the net radiative heat flux (W/m^2) , respectively.

Moreover, $h_{net,c}$ is determined by

$$h_{net,c} = \alpha_c \left(T_g - T_a \right) \tag{3}$$

where α_c is the coefficient of convective heat transfer, which is taken as 25W/(m^2°C) here for the standard temperature-time curve; T_g is the gas temperature (°C); and T_a is the surface temperature of the steel member (°C).

Meanwhile, $h_{net,r}$ is given by

$$h_{net,r} = \Phi \varepsilon_m \varepsilon_f \sigma \left[\left(T_r + 273 \right)^4 - \left(T_a + 273 \right)^4 \right] \tag{4}$$

where, Φ is the configuration factor, which is usually 1.0; ε_m is the surface emissivity of the member, which is 0.7 for carbon steel; ε_f is the emissivity of gas, which is 1; σ is the Stefan-Boltzmann constant, which is 5.67×10^{-8} W/(m^2·°C); and T_r is the environment temperature, which is T_g in the case of fully surrounded members.

4.1.2. CECS200 Equation

The equation suggested by CECS200 is:

$$T_a \left(t + \Delta t \right) = \frac{B}{c_a \rho_a} \left[T_g \left(t \right) - T_a \left(t \right) \right] \Delta t + T_a \left(t \right) \tag{5}$$

where B is the comprehensive heat transfer coefficient [W/(m^3·°C)], given by

$$B = \left(\alpha_c + \alpha_r \right) \frac{A_m}{V} \tag{6}$$

where α_r is the radiation heat transfer coefficient [W/(m^2·°C)], given by

$$\alpha_r = \frac{2.041}{T_g - T_a} \left[\left(\frac{T_g + 273}{100} \right)^4 - \left(\frac{T_a + 273}{100} \right)^4 \right] \tag{7}$$

4.2. Temperature Calculation and Comparison

The temperature-time curves for steel beams obtained by Eqs. (1) and (5) are compared with the experimental curves. The parameters used in the equations adopt the values suitable for standard fires. For simplicity, this manuscript only provides temperature-time curves of some representative measuring points, as shown in Fig. 24. The letters “C” and “E” mean that the corresponding temperature-time curves of steel members are obtained by the equations in CECS200 and EN 1993-1-2, respectively. As mentioned in Section 2, “S” and “G” mean that the curves are derived from steel members and hot gas respectively in the fire test.

It can be seen from Fig. 24 that the curves given by the equations of the two codes are very close to each other. The curves plotted in Figs. 24(a)-(d)

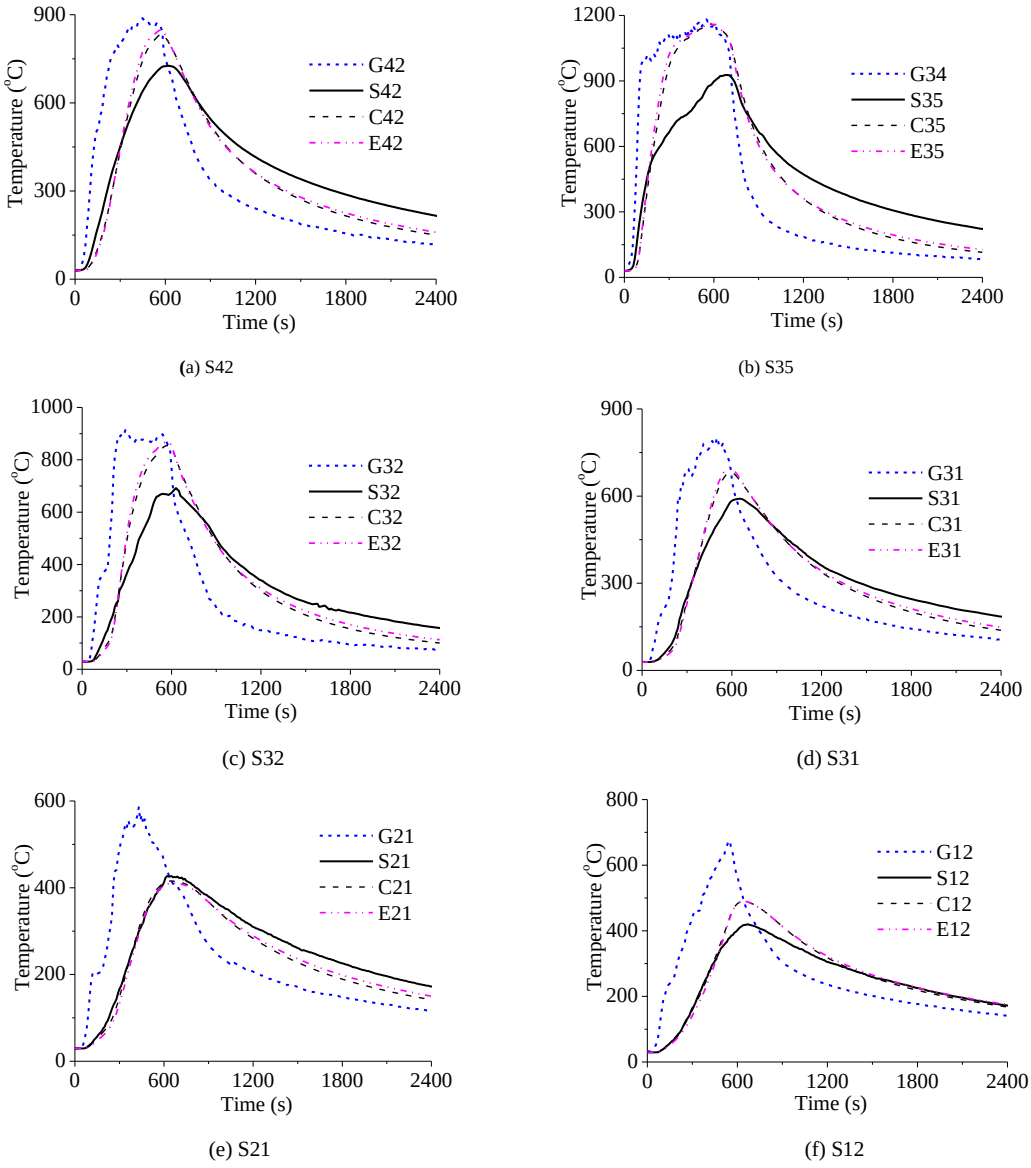

Fig. 24 Comparison of experimental and calculation curves

are obtained from measuring points in the flame or the high-temperature zone of the hot gas layer. The calculation results are in satisfactory agreement with the experimental results during the heating period. However, after the temperature is higher than 600ºC, the calculation results are higher than the experimental results, while the calculation results decrease faster than the experimental results during the cooling period.

Figs. 24(e)-(f) show results from measuring points in the slightly lower-temperature zone of the hot gas layer. The calculation and experimental curves of the measuring point S21 are very close to each other in the heating period, whereas the calculation curves have steeper downward slopes than the experimental curves during the cooling period. For the measuring point S12, the calculation results agree well with the experimental results during the heating period and the cooling period, but the calculation results are higher than the experimental results near the peak temperature.

Due to the fact that the calculation results from these representative measuring points are close to or higher than the experimental results during the heating period, the additional thermal radiation effect of the flame can be omitted in the calculation of the temperature of the steel beam within the hot gas layer. It also means that the thermal radiation heat from the flame is completely absorbed by the upper hot gas layer.

4.3. Modified Model and Calculation Comparison

To solve the problem of the difference between the calculation results from the equations and the experimental results, this manuscript proposes a modified equation based on the one specified by EN 1993-1-2. The coefficients of convection and radiation are modified through the regression analysis of the experimental data. The new form of the calculation equation for natural fires is described below:

$$T_a = k_{sh}\frac{A_m/V}{c_a\rho_a}\left\{\alpha_c\left(T_g - T_a\right) + \varepsilon_{mg}\sigma\left[\left(T_g+273\right)^4 - \left(T_a+273\right)^4\right]\right\}\Delta t \quad (8)$$

where ε_{mg} is the comprehensive radiation coefficient. During the heating period, α_c is 25W/(m²·ºC); ε_{mg} is 0.7 when $T_a \leq 600$ºC and 0.07 when $T_a > 600$ºC; and during the cooling period, α_c is 12.5W/(m²ºC) and ε_{mg} is 0.49.

The new results calculated by Eq. (8) are compared to those by the original equation specified by EN 1993-1-2 and to the experimental data, as plotted in Fig. 25. In these figures, the curves from the new equation with correction parameters are represented by the letter “N”. It can be seen from Figs. 25(a)-(e) that the new calculation results are very close to the experimental results. Table 1 shows the comparison of peak temperatures between calculation and experimental results, at the measuring points S42, S35, S32 and S31. The calculation errors from EN 1993-1-2 and the revised equation were 16.9%~25.6% and -2.4%~8.5%, respectively. Therefore, the calculation accuracy is evidently improved due to the correction parameters. In terms of the measuring point S12, as shown in Fig. 25(f), the calculation results from the proposed equation are slightly higher than the experimental results during the cooling period. The reason is that the calculation results have been higher than the experimental results before the beginning of temperature decline. However, they have the similar decline rates. On the whole, the proposed equation with the correction parameters can accurately predict the temperature variations of steel beams during the whole process of natural fires. Note that there is more work to be done to give equations that can be applied universally.

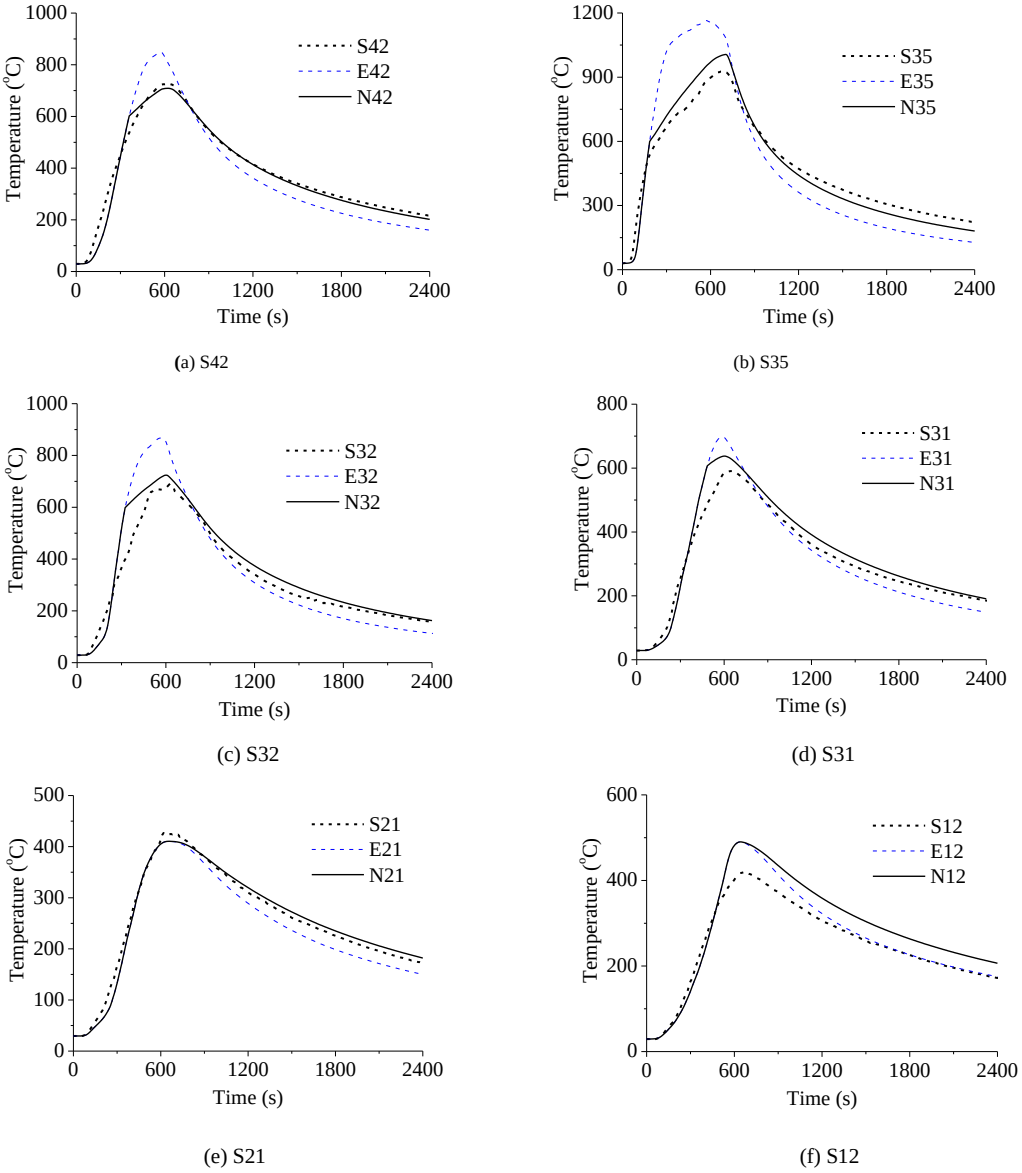

Fig. 25 New comparison of experimental and calculation curves

Table 1
Comparison of peak temperatures between calculation and experimental results

Measuring point	S/°C	E/°C	Error(E)	N/°C	Error(N)
S42	725.9	848.5	16.9%	708.8	-2.4%
S35	927.3	1164.5	25.6%	1006.4	8.5%
S32	692.1	867.3	25.3%	724	4.6%
S31	590.7	699	18.3%	637.4	7.9%

Notes: S is the experimental result of the peak temperature of the steel member; E and N are the calculation results of the peak temperature obtained by Eq. (1) and Eq. (8), respectively.

5. Conclusions

In this study, a model of a portal frame building was designed and constructed to perform a natural fire test. The temperature development of the hot gas layer and the steel beams inside the model was investigated. The equations specified by EN 1993-1-2 and CECS200 were adopted to calculate the temperature of the steel members. The calculation results were then compared to the experimental results. Meanwhile, some related parameters were modified to obtain more accurate calculation results based on the equation specified by EN 1993-1-2. The following conclusions can be drawn:

a) The temperature-time history of the hot gas above the fire source had three periods, including a growth period, a fully developed period, and a decay period. The peak temperature of the hot gas gradually decreased from the region directly above the fire source to the neighbouring regions. On the whole, the temperature symmetrically distributed along both sides of the roof ridge.

b) The entire temperature-time history of the steel beam showed apparent thermal hysteresis compared to that of the hot gas. Moreover, the temperature distribution of steel members was roughly uniform over the cross-section while non-uniform along the length direction. The experiment showed that the peak temperatures of the hot gas and steel beams were 1182.7°C and 941°C, respectively.

c) The calculation results for the temperature of steel beams given by the equations in EN 1993-1-2 and CECS200 were very similar. However, during the heating period, these calculation results were much higher than the experimental results after the temperature of the steel beam reached 600°C. Meanwhile, the predicted results had a higher decline rate than the experi-

mental results during the cooling period. Thus, the effect of thermal radiation from the flame can be ignored in the calculation of the temperature of the steel beam within the hot gas layer.

d) To accurately acquire the temperature-time curves of steel beams subjected to natural fires, the present study proposes a modified method based on EN 1993-1-2, through modifications to the coefficients of convection and radiation. It can be found that the proposed method leads to more accurate results than those obtained by EN 1993-1-2.

References

[1] Luo B., Sun Y., Guo Z.X. and Pan H.T., "Multiple random-error effect analysis of cable length and tension of cable-strut tensile structure", Advances in Structural Engineering, 19(8), 1289-1301, 2016.

[2] Tong G.S., Pi Y.L. and Gao W., "In-plane nonlinear analysis and buckling of shear-deformable circular arches", Advanced Steel Construction, 16(1), 55-64, 2020.

[3] Xue S.D., Lu J., Li X.Y. and Liu R.J., "Improved force iteration method based on rational shape design solving self-stress modes of cable-truss tensile structure", Advanced Steel Construction, 16(2), 170-180, 2020.

[4] Yan X.Y., Hu H., Chen Z.H. and Yang Y., "An improved mathematical calculation method for beam string structure based on static equilibrium principle", International Journal of Steel Structures, 20(4), 1241-1255, 2020.

[5] Lu L.M., Yuan G.L., Huang Z.H., Shu Q.J. and Li Q., "Performance-based analysis of large steel truss roof structure in fire", Fire Safety Journal, 93, 21-38, 2017.

[6] Du Y., Liew J.Y.R., Zhang H. and Li G.Q., "Pre-tensioned steel cables exposed to localised fires", Advanced Steel Construction, 14(2), 206-226, 2018.

[7] Woźniczka P., "Fire resistance assessment of the long-span steel truss girder", Archives of Civil Engineering, LXVI(2), 63-75, 2020.

[8] Liu H.B., Zhang Y.J., Wan L. and Chen Z.H., "Mechanical performance of welded hollow spherical joints at elevated temperatures", Advanced Steel Construction, 16(1), 1-12, 2020.

[9] Jiang S.C., Zhu S.J., Guo X.N. and Li Z.Y., "Full-scale fire tests on steel roof truss structures", Journal of Constructional Steel Research, 169, 1-13, 2020.

[10] Pyl L., Schueremans L., Dierckx W., and Georgieva I., "Fire safety analysis of a 3D frame structure based on a full-scale fire test", Thin-Walled Structures, 6, 204-212, 2012.

[11] Johnston R.P.D., Lim J.B.P., Lau H.H., Xu Y.X., Sonebi M., Armstrong C.G. and Mei C.C., "Finite-element investigation of cold-formed steel portal frames in fire", Structures and Buildings, 169(SB1), 3-9, 2015.

[12] Lou G.B., Wang C.H., Jiang J., Jiang Y.Q., Wang L.W. and Li G.Q., "Experimental and numerical study on thermal-structural behavior of steel portal frames in real fires", Fire Safety Journal, 98, 48-62, 2018.

[13] Lou G.B., Wang C.H., Jiang J., Jiang Y.Q., Wang L.W. and Li G.Q., "Fire tests on full-scale steel portal frames against progressive collapse", Journal of Constructional Steel Research, 145, 137-152, 2018.

[14] Roy K., Lim J.B.P., Lau H.H., Yong P.M., Clifton G.C., Johnston R.P.D., Wrzesien A. and Mei C.C., "Collapse behaviour of a fire engineering designed single-storey cold-formed steel building in severe fires", Thin-Walled Structures, 142, 340-357, 2019.

[15] Milke J.A., "Performance-based analysis methods to determine the fire resistance of structural members", Proceedings of the 2001 Structures Congress and Exposition, Washington, D.C., United States , 1-11, 2001.

[16] Shi Y.J., Bai Y. and Wang Y.Q., "Study on performance-based fire-resisting design and key technologies for large spatial steel structures", Engineering Mechanics, 23(Sup. II), 85-92, 2006.

[17] CECS200, Technical code for fire safety of steel structures in buildings, China Association for Engineering Construction Standardization, Beijing, China, 2006.

[18] EN1991-1-2, Eurocode1: Actions on structure. Part 1-2: General actions-Actions on structures exposed to fire, European Committee for Standardization, Brussels, Belgium, 2002.

[19] EN1993-1-2, Eurocode 3: Design of steel structures. Part 1-2: General rules-Structural fire design, European Committee for Standardization, Brussels, Belgium, 2005.

[20] Latham D.J., Kirby B.R. and Thomson G., "The temperatures attained by unprotected steelwork in experimental natural fires", Fire Safety Journal, 12, 139-152, 1987.

[21] Wong M.B., Ghojel J.I. and Grozier D.A., "Temperature-time analysis for steel structures under fire conditions", Structural Engineering and Mechanics, 6(3), 275-289, 1998.

[22] Ghojel J.I., "A new approach to modelling heat transfer in compartment fires", Fire Safety Journal, 31, 227-237, 1998.

[23] Wald F., Chladná M., Moore D., Santiago A. and Lennon T., "Temperature distribution in a full-scale steel framed building subject to a natural fire", Steel and Composite Structure, 6 (2), 159-182, 2006.

[24] Wald F., Chlouba J., Uhlír A., Kallerová P. and Štujberová M., "Temperatures during fire tests on structure and its prediction according to Eurocodes", Fire Safety Journal, 44, 135-146, 2009.

[25] Du Y. and Li G.Q., "Fire radiation effect on steel member at elevated temperature in large space fire", Fire Safety Science, 15(4), 189-199, 2006.

[26] Huang J.Q., Li G.Q., Du Y., Bao P.Q. and Liu K., "Influence of flame radiation on temperature rising of steel members in large space fire", Journal of Natural Disasters, 17(5), 87-94, 2008.

[27] Zhang C., Li G.Q. and Wang R.L., "Using adiabatic surface temperature for thermal calculation of steel members exposed to localized fires", International Journal of Steel Structures, 13(3), 547-556, 2013.

[28] Zhang G.W., Zhu G.Q. and Huang L.L., "Temperature development in steel members exposed to localized fire in large enclosure", Safety Science, 62(3), 319-325, 2014.

[29] McGrattan K., Hostikka S., Floyd J., McDermott R. and Vanella M., Fire Dynamics Simulator User's Guide (Version 6), National Institute of Standards and Technology (NIST), Maryland, 2015.

Acknowledgments

The research work described in this paper is sponsored by the Nation Science Foundation of China (Grant No. 51808117), the Fundamental Research Funds for the Central Universities (Grant No. 2242020K40088) and the National Key Research and Development Program of China (Grant No. 2018YFC0705502-4). Their financial support is highly appreciated.